Stability of Oil-in-Water Emulsions in a Low Interfacial Tension System

B. P. Binks,* W−G. Cho, P. D. I. Fletcher, and D. N. Petsev†

Surfactant Science Group, Department of Chemistry, University of Hull, Hull HU6 7RX, U.K.

Received July 19, 1999. In Final Form: October 4, 1999

The stability of oil-in-water emulsions to both creaming and coalescence was measured as a function of salt concentration in heptane + water mixtures stabilized by sodium bis(2-ethylhexylsulfosuccinate) (AOT). Emulsions were prepared from pre-equilibrated phases in Winsor I systems. Up to 0.035 M NaCl, the creaming rate decreases with salt concentration, with no visible sign of coalescence. Above 0.035 M and approaching the phase inversion salt concentration of 0.055 M, the creaming rate increases quite markedly and coalescence becomes appreciable. The creaming at low salt concentrations is due mainly to the buoyancy motion of single drops. A simple model for the time evolution of resolved water is developed which successfully describes the behavior. The drop size changes observed are shown to be due to Ostwald ripening, the rate of which decreases with salt concentration. Experimental ripening rates are consistent with a mechanism by which oil is transported between emulsion drops via microemulsion droplets present in the continuous phase. We calculate the energy of interdrop interaction allowing for drop deformation using experimentally determined parameters of interfacial tension, drop radius, and zeta potential. At high [NaCl], due mainly to the low interfacial tension, the drops can deform and the attraction between them becomes significant. As a result, flocculation occurs which leads to coalescence instability.

Introduction

Macroemulsions composed of drops in the micron-size range are not thermodynamically stable and there are various sources of instability leading ultimately to phase separation.[1] Creaming or sedimentation of drops can occur depending on the density difference between the dispersed and continuous phases and can be enhanced or restricted by flocculation. Ostwald ripening is the growth of large drops at the expense of smaller ones and relies on the transport and solubility of the dispersed phase in the continuous phase. For coalescence to occur, the thinning film between approaching drops must reach a critical thickness. Emulsion type and stability are known to be associated with the equilibrium phase behavior in surfactant + oil + water systems.[2−6] The hydrophile−lipophile balance (HLB) of the system (as opposed to the empirical HLB number of the surfactant) is related to the locus of aggregate formation in equilibrated mixtures. High HLB systems are those in which aqueous micelles or oil-in-water (o/w) microemulsion droplets form i.e., Winsor I systems. Low HLB systems are Winsor II systems where reverse micelles in oil or water-in-oil (w/o) microemulsion droplets exist. It is frequently observed that the type of emulsion (o/w or w/o) formed by homogenization of the Winsor system is the same as that of the equilibrium microemulsion, i.e., emulsification of an o/w microemulsion plus excess oil gives an o/w emulsion. Why this is the case has been discussed by Petsev et al.[7] and Kabalnov and Wennerström[8] who argue the correspondence in terms of interfacial bending energies and monolayer curvature.

Unlike dispersions of solid particles whose behavior and stability is usually satisfactorily explained in the framework of the Derjaguin−Landau−Verwey−Overbeek (DLVO) theory, emulsions are more complex because the drops can deform and because the surfaces are fluid. These two effects have a great impact on the intermolecular and hydrodynamic interactions between fluid particles. It has been established that when two large drops of millimeter size approach each other, they deform and a planar film forms between them.[9] The rate of thinning and the stability against rupture of this film determines the overall stability to coalescence of the emulsion. Until recently it was not clear whether such deformation took place when smaller drops (of micron size) are considered. On one hand smaller drops possess higher capillary pressure which opposes their deformation; on the other hand they undergo intensive Brownian motion giving rise to an additional force enhancing the deformation. When a film of small radius is present, the pair interaction cannot be described by theories for either infinite planar films or for spheres, because the contribution of the spherical parts to the interaction is comparable to that of the film. Danov et al.[10,11] have considered in detail the pair interaction energy between two, small deformable drops. Explicit expressions for the van der Waals interaction are derived using the Hamaker approach, and the other types of interaction including electrostatic and steric are treated by applying Derjaguin's method to slightly deformed spheres. The influence of the deformation on the interaction energy depends crucially on the charge on the drop interfaces

* To whom correspondence should be addressed. E-mail: b.p.binks@chem.hull.ac.uk.

† Present address: Centre for Microgravity and Materials Research, University of Alabama in Huntsville, Huntsville, AL 35899

(1) Binks, B. P. In *Modern Aspects of Emulsion Science*; Binks, B. P., Ed.; The Royal Society of Chemistry: Cambridge, 1998, pp 1−55.

(2) Baldauf, L. M.; Schechter, R. S.; Wade, W. H.; Graciaa, A. *J. Colloid Interface Sci.* **1982**, *85*, 187.

(3) Anton, R. E.; Salager, J.-L. *J. Colloid Interface Sci.* **1986**, *111*, 54.

(4) Aveyard, R.; Binks, B. P.; Fletcher, P. D. I.; Ye, X.; Lu, J. R. In *Emulsions—A Fundamental and Practical Approach*; Sjöblom, J., Ed.; Kluwer: Amsterdam, 1992, p 97.

(5) Binks, B. P. *Langmuir* **1993**, *9*, 25.

(6) Binks, B. P.; Dong, J.; Rebolj, N. *Phys. Chem. Chem. Phys.* **1999**, *1*, 2335.

(7) Petsev, D. N.; Denkov, N. D.; Kralchevsky, P. A. *J. Colloid Interface Sci.* **1995**, *176*, 201.

(8) Kabalnov, A.; Wennerström, H. *Langmuir* **1996**, *12*, 276.

(9) Ivanov, I. B. *Pure Appl. Chem.* **1980**, *52*, 1241.

(10) Danov, K. D.; Petsev, D. N.; Denkov, N. D.; Borwankar, R. *J. Chem. Phys.* **1993**, *99*, 7179.

(11) Denkov, N. D.; Petsev, D. N.; Danov, K. D. *Phys. Rev. Lett.* **1993**, *71*, 3226.

10.1021/la990952m CCC: $19.00
Published on Web 11/20/1999

and on the interfacial tension; if repulsion exists the drops behave as hard spheres and deformation is impossible. Deformation sets in at larger separations when the tension is lowered. No experimental verification of these ideas has so far been published.

In this paper we investigate the stability of heptane-in-water (o/w) emulsions stabilized by the anionic surfactant sodium bis(2-ethylhexylsulfosuccinate) (AOT) as a function of salt concentration. The emulsions are prepared from the corresponding Winsor I systems, i.e., by mixing an o/w microemulsion phase with an excess oil phase. This system is carefully chosen because the oil−water interfacial tension reaches ultralow values approaching the phase inversion salt concentration[12] and hence the possibility of drop deformation setting in is enhanced. We account for the stability to creaming at low [salt] using a simple hydrodynamic model and the added effect of Ostwald ripening. At higher [salt], we calculate the total pair interaction energy between drops using available experimental parameters and show why coalescence is more likely as observed.

Experimental Section

Materials. Water was passed through a reverse osmosis unit and then a Milli-Q reagent water system. Water treated in this way had a surface tension of 71.9 ± 0.1 mN m^{-1} at 25 °C in good agreement with the best literature values. *n*-Heptane of 99% purity was purchased from Fisons Spectrograde and was passed twice through chromatographic alumina to remove traces of polar impurities. The surfactant AOT was obtained from Sigma (99%) and was used as received. The electrolyte was AnalaR grade sodium chloride from Prolabo. All glassware was washed in chromic acid, rinsed in hot water, and then rinsed with ultrapure water.

Methods. *Equilibrium Phase Behavior*. This was determined by preparing mixtures of equal volumes of aqueous electrolyte solution and heptane. The AOT was initially dissolved in the water phase at a concentration of 40 mM. The glass tubes were shaken thoroughly and left to equilibrate in a thermostat at 25 °C until phase separation was complete.

Oil−Water Interfacial Tensions. Interfacial tensions γ at the heptane−water interface were measured by the spinning drop technique using a Krüss Site 04 tensiometer. A drop of pure heptane was put in contact with an aqueous phase containing 40 mM AOT and γ reached equilibrium within 15 min. The densities and refractive indices of the oil and aqueous phases required for the calculation of γ were measured at 25 °C using a Paar DMA 55 densimeter and an Abbé refractometer, respectively.

Preparation, Conductivity and Stability of Emulsions. Two sets of o/w emulsions were prepared. In the first set (method 1), the pre-equilibrated phases (consisting of an o/w microemulsion plus excess oil phase) prepared as described above were mixed. Here, the salt concentration within the emulsion is set by the initial concentration in water. As seen later, the average emulsion drop size, however, varies with salt concentration. To separate the effects of changing drop size and added salt on emulsion stability, a second set of emulsions (method 2) was prepared from a single stock emulsion. Five volumes of heptane and 4 volumes of 40 mM aqueous AOT containing 0.005 M NaCl were mixed gently and left to equilibrate. After homogenization, the stock emulsion was divided into 9 cm^3 samples and loaded into graduated glass tubes containing 1 cm^3 of different concentrations of aqueous NaCl and surfactant at the respective critical micelle concentration (cmc). Each tube was gently inverted a number of times in order to disperse the salt solution into the emulsions. In this way, it was verified that all emulsions were of the same size distribution initially so that changes in stability could be ascribed only to the effect of added salt. The homogenization of both sets of emulsions was performed using a Janke and Kunkel ultra-turrax T25 homogenizer with shaft 18G operating at 8000 rpm for 3 min.

Emulsion type was detected using conductivity measurements. Immediately after preparation, the conductivities were measured at 25 °C using a digital conductivity meter (Jenway PCM3). Because the conductivity of o/w and w/o emulsions differs by several orders of magnitude, phase inversion of the emulsions is readily observable. Emulsion stability was assessed by monitoring the positions of the various interfaces between macroscopic phases with time. For the o/w emulsions, creaming resulted in the appearance of a clear aqueous layer beneath the emulsion (water/emulsion interface) and coalescence produced a clear oil phase above the emulsion (oil/emulsion interface).

Emulsion Drop Size Distribution Measurement. Drop size distributions (either by number or by volume) were determined using a Malvern 2600c diffractometer of resolution 1 μm for both fresh emulsions and for aged emulsions. Typically, two or three drops (0.1 cm^3) of emulsion were diluted into approximately 200 cm^3 of water containing AOT at a concentration equal to the cmc and at a salt concentration equal to that of the parent emulsion. This was to ensure that no desorption of surfactant from the emulsion drop surfaces occurred in the dilution procedure. The sizing was performed at ambient temperature (22 °C).

Measurement of Mobility of Emulsion Drops. The electrophoretic mobilities of o/w drops were determined as a function of salt concentration for dilute emulsions using a Rank Brothers MK II microelectrophoresis instrument. The zeta potential ζ of the drops is linearly proportional to the mobility u via[13]

$$\zeta = \frac{\eta u}{\epsilon_0 \epsilon} \frac{1}{f(\kappa a)} \tag{1}$$

where η is the viscosity of the solvent, ϵ and ϵ_0 are the relative dielectric permittivity and the permittivity of free space, respectively, and $f(\kappa a)$ is a function accounting for the electrophoretic retardation, in which a is the drop radius and κ is the inverse Debye length, which for monovalent electrolyte is

$$\kappa = \left(\frac{2e^2 c_{el}}{\epsilon_0 \epsilon kT}\right)^{0.5} \tag{2}$$

where e is the electron charge, c_{el} is the electrolyte concentration, and kT is the thermal energy. An expression for $f(\kappa a)$ suggested recently by Ohshima[14] has the following form

$$f(\kappa a) = \frac{2}{3}\left\{1 + \frac{1}{2}\left[1 + \frac{5}{2\kappa a}(1 + 2\exp(-\kappa a))\right]^3\right\} \tag{3}$$

and is accurate to within 1% for the entire range of values of the product κa. The concentration of monomeric surfactant (present in the continuous phase of the emulsion at a concentration equal to the cmc) was taken into account in calculating κ.

Results and Discussion

(a) Phase Behavior and Emulsion Stability Versus [NaCl]. The equilibrium phase behavior of the AOT−aqueous NaCl−heptane system at 25 °C is as follows (Figure 1a). At 40 mM surfactant (approximately 17 times the cmc in pure water) two phases coexist at salt concentrations between 0 and 0.05 M NaCl. They are an o/w microemulsion phase and an excess oil phase (Winsor I system). The solubilization of heptane into the aqueous aggregates increases progressively with [NaCl] until three phases appear at 0.055 and 0.06 M NaCl (Winsor III system) with the aggregated surfactant forming the third phase. Above 0.06 M NaCl, two phases are formed (Winsor II system) consisting of a w/o microemulsion and an excess aqueous phase. Emulsification of the coexisting phases shows that the emulsions are highly conducting and hence

(12) Aveyard, R.; Binks, B. P.; Mead, J. *J. Chem. Soc., Faraday Trans. 1*, **1986**, *82*, 1755.

(13) Hunter, R. J. *Zeta Potential in Colloid Science*; Academic Press: London, 1981.

(14) Ohshima, H. *J. Colloid Interface Sci.* **1994**, *168*, 269.

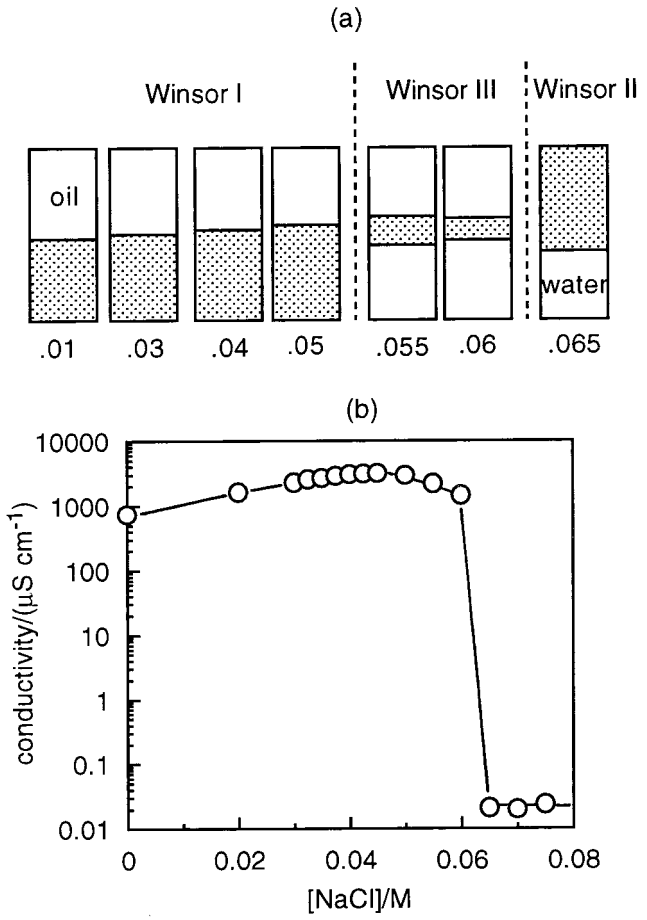

Figure 1. (a) Phase sequence after 1 week for the system: 40 mM AOT in aqueous NaCl + heptane (1:1 v/v) at 25 °C. Dashed lines enclose the three-phase region and the shaded areas indicate the location of aggregated surfactant. Numbers are [NaCl]/M. (b) Conductivity of emulsions prepared from the equilibrium phases in (a) versus salt concentration.

o/w in Winsor I systems, and invert to nonconducting and hence w/o in Winsor II systems (Figure 1b). The three-phase emulsions are also conducting but it is difficult to speculate on the nature of the continuous phase in this case.

Figure 2 shows that in Winsor I systems the equilibrium o/w microemulsion−heptane interfacial tension γ falls to very low values ($<10^{-3}$ mN m^{-1}) at salt concentrations close to the Winsor I/III boundary, after which it rises again. Concomitant with this lowering is the fact that the initial volume average diameter, d (v, 0.5), of the o/w emulsions prepared from Winsor I systems decreases on the addition of salt up to around 0.035 M, after which it rises quite sharply. We will see later that the initial decrease follows from an increasing ease of emulsification as the tension falls, and that the size increase above 0.04 M NaCl is a result of instability that is probably due to coalescence.

The effect of salt concentration on the stability to creaming of o/w emulsions is shown in Figure 3. For low [NaCl] in the range 0−0.02 M, the resolution of the aqueous phase is fast. At intermediate [NaCl] between 0.025 and 0.04 M, there is a long induction period before any creaming occurs of between 20 and 45 h. The creaming rate passes though a minimum in the same range of salt concentration. At high [NaCl] beyond 0.04 M the creaming rate increases again. Figure 4a shows the evolution of the volume average diameter of the emulsions with time at various [NaCl]. These emulsions were prepared from

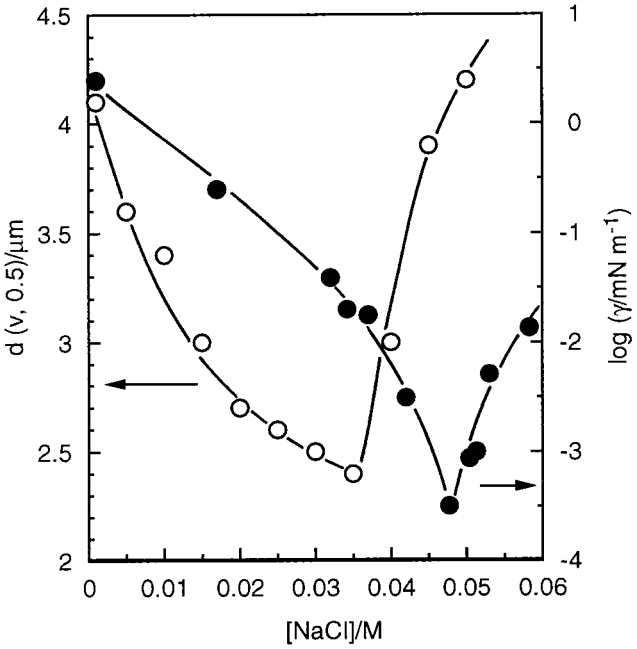

Figure 2. Variation of initial volume average diameter of o/w emulsions (left-hand ordinate) and interfacial tension (right-hand ordinate) with salt concentration.

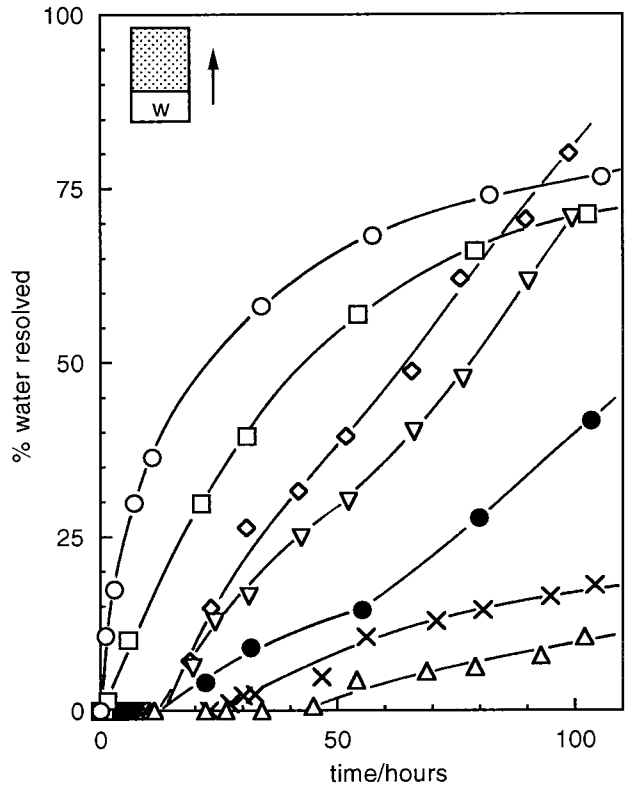

Figure 3. Resolution of aqueous phase (creaming) with time for o/w emulsions for different initial salt concentrations. The [NaCl]/M are 0 (open circles), 0.01 (squares), 0.025 (filled circles), 0.035 (triangles), 0.04 (crosses), 0.0425 (inverted triangles), and 0.05 (diamonds). The arrow refers to the direction of movement of the water-emulsion interface.

equilibrium phases in which the salt was added initially (method 1). As a result, the initial diameter varies with salt concentration but the change with time decreases on increasing [NaCl] such that by 0.035 M NaCl the drop size remains virtually constant. The decreasing rate of change of drop size with time between 0 and 0.035 M

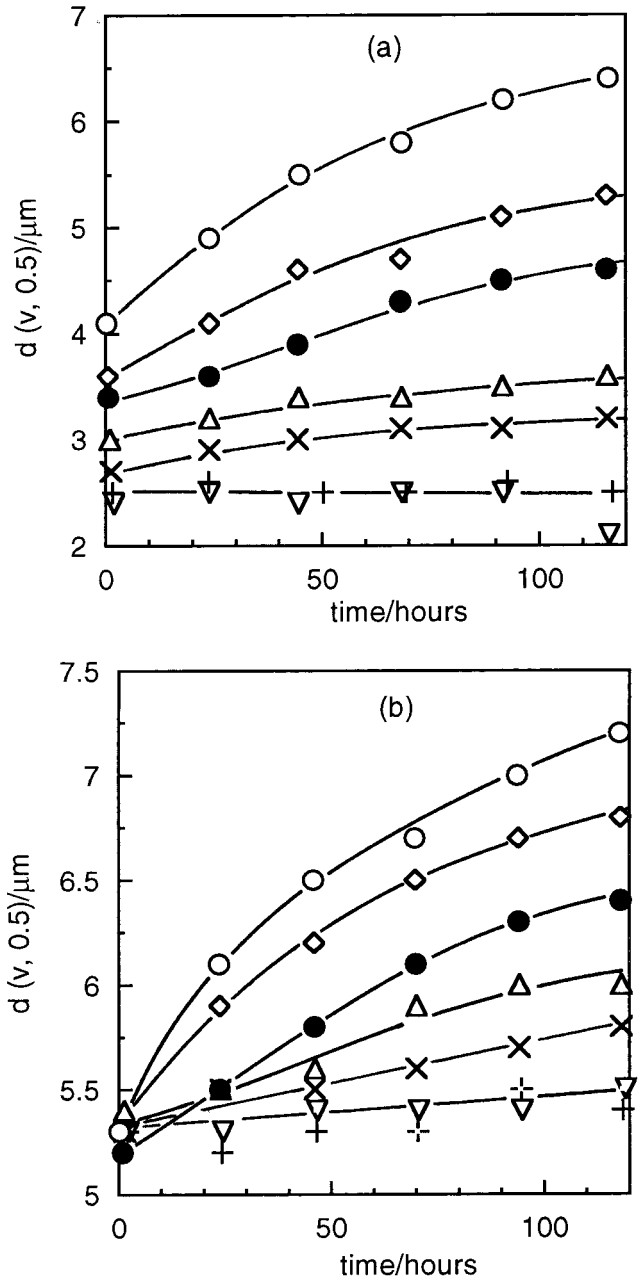

Figure 4. (a) Change in volume average diameter with time for o/w emulsions for different initial salt concentrations (method 1). The [NaCl]/M are 0 (open circles), 0.005 (diamonds), 0.01 (filled circles), 0.015 (triangles), 0.02 (crosses, x), 0.03 (crosses, +), and 0.035 (inverted triangles). (b) As for (a) but for emulsions prepared by method 2.

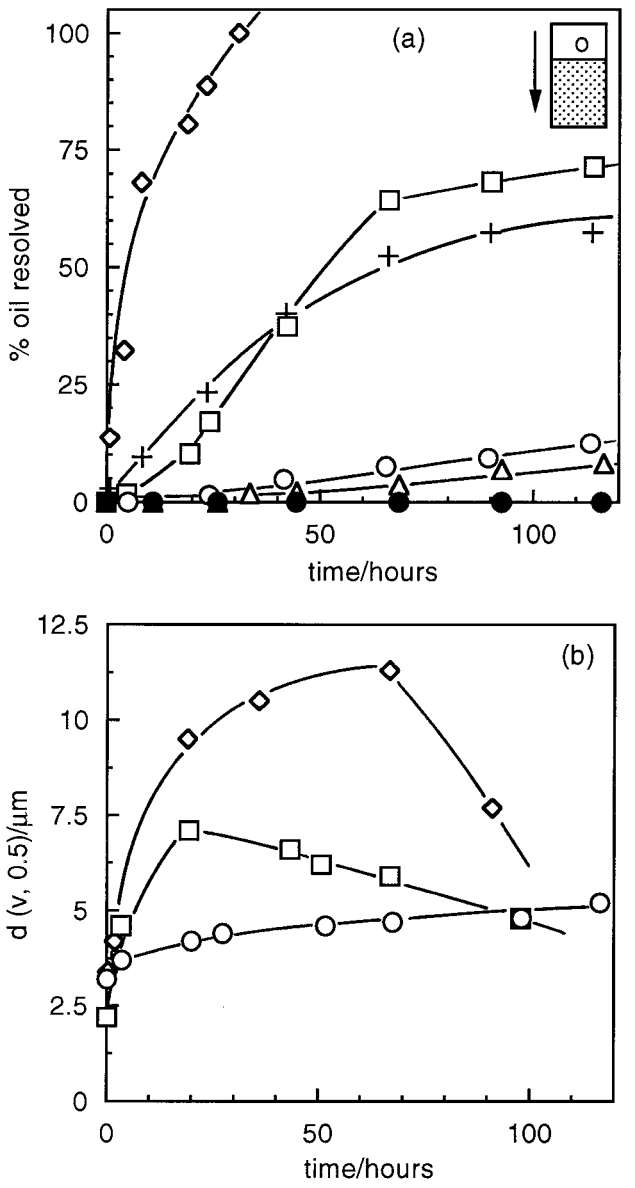

Figure 5. (a) Resolution of oil phase (coalescence) with time for o/w emulsions for different initial salt concentrations. The [NaCl]/M are 0.035 (filled circles), 0.0375 (triangles), 0.04 (open circles), 0.0425 (squares), 0.045 (crosses), and 0.05 (diamonds). The arrow refers to the direction of movement of the oil−emulsion interface. (b) Change in volume average diameter of same emulsions with time. Symbols as in (a).

NaCl is in line with a decrease in the rate of creaming, because creaming velocity in dilute systems is proportional to the square of the radius. To investigate the effect of salt on the stability of emulsions in the absence of complications due to varying drop size, emulsions of fixed initial drop size were prepared by adding the appropriate concentration of salt to aliquots of a stock emulsion (method 2). Figure 4b shows the time variation of the average diameter where it can be seen that the trend with [NaCl] is similar to that reported above. The conclusion is that the change in d (v, 0.5) with time is dominated by an intrinsic effect of the salt and is less likely due to any differences in the initial drop size distributions.

Below 0.035 M NaCl, coalescence is thought to be negligible because the percentage of oil resolved at times of up to 150 h is zero. Figure 5a shows the resolution of heptane with time for emulsions containing between 0.035 and 0.05 M NaCl prepared by method 1. On approaching the Winsor I/III boundary the oil resolution rate increases rapidly. The induction period decreases substantially such that at 0.05 M NaCl all the oil is resolved within 30 h. The variation of the average drop diameters with time are given in Figure 5b for three [NaCl]. The size increases initially and then levels off for 0.04 M. At 0.045 and 0.05 M, the initial size increase is larger and the apparent size decreases at longer times. The decrease is thought to be a result of loss of the larger drops by coalescence to give a separate oil phase causing the distribution of sizes in the remaining emulsion to be shifted to smaller size. This was confirmed by careful inspection of the drop size distributions. As in the case of the creaming experiments, we examined coalescence in emulsions prepared from a stock emulsion of fixed average diameter (method 2). The resolution of oil and the drop size changes observed (not

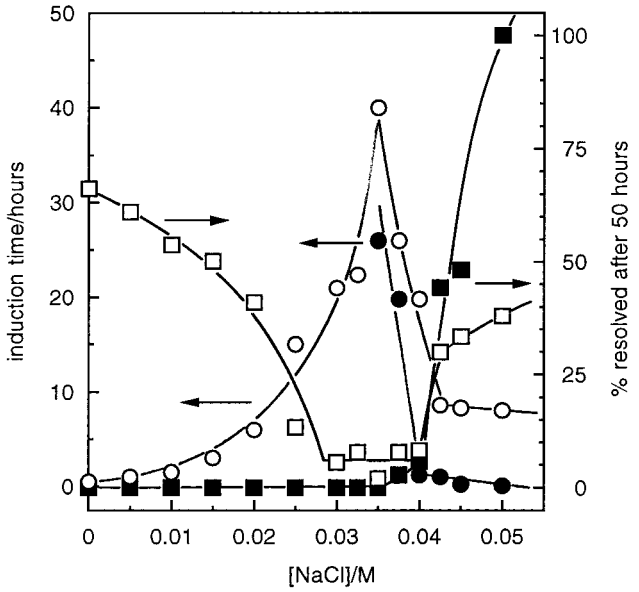

Figure 6. Summary of stability of o/w emulsions with salt concentration. Left-hand ordinate refers to the induction time for water resolution (open circles) and oil resolution (filled circles). Right-hand ordinate refers to the percentage of phase resolved after 50 h for water (open squares) and for oil (filled squares).

shown) follow the same pattern of behavior as for the emulsions prepared by method 1.

The basic observations regarding the stability of o/w emulsions as a function of salt concentration are summarized in Figure 6. Upon increasing [NaCl] the induction time for the resolution of water increases, reaches a maximum around 0.035 M, and then decreases. The induction time for the appearance of oil is infinite below 0.035 M, and decreases above this. The percentage of water resolved after 50 h decreases initially, reaches a minimum around 0.035 M, and then increases again. The percentage of oil resolved begins to increase markedly at 0.04 M. Thus, a well-defined minimum in the creaming rate occurs at 0.035 M NaCl. Below this no coalescence occurs, whereas above it coalescence is appreciable. For emulsions stabilized by ionic surfactants, it has been reported that an increase in salt concentration causes flocculation by screening the double layer repulsions between drops which in turn enhances creaming.[15] It is clear in the present system that an opposite effect prevails below 0.035 M NaCl, i.e., creaming is reduced in the presence of salt.

In the next two sections we attempt to explain the experimental results within the framework of a uniform and consistent physical picture. Depending on the salt concentration, we suggest that three different phenomena contribute to the emulsion stability. At low concentrations of electrolyte, creaming is enhanced as a result of Ostwald ripening and is governed primarily by the buoyancy motion of single drops. At high concentrations of salt however, flocculation leading to coalescence occurs. Flocculation depends on the variation of both the oil−water tension and the Debye screening length and is predicted theoretically.

(b) Stability at Low [NaCl], ≤ 0.035 M. We discuss the creaming at low [NaCl] using a simple model. In these cases, drop flocculation and coalescence are assumed to be suppressed due to the electrostatic repulsion. A second assumption is that the drop concentration is considered uniform within the volume containing the emulsion above the resolved water. The kinetics of creaming is then governed by the upward motion of the drops, driven by the density difference between oil and water. The high-volume fraction, ϕ, of the emulsion drops (initially equal to 0.5) implies that there are considerable hydrodynamic interactions between the drops. Hence, the creaming velocity, v, of a drop is given by[16]

$$v = \frac{a^2 \Delta\rho g}{3\eta\varphi(\phi)} \tag{4}$$

where a is the (initial) drop radius, $\Delta\rho$ is the density difference between oil and water, g is the acceleration due to gravity, η is the continuous phase viscosity, and $\varphi(\phi)$ accounts for the interdrop hydrodynamic interactions. The velocity of a single drop colliding with the air−emulsion surface is

$$v = H\frac{\mathrm{d}L'}{\mathrm{d}t} = \frac{a^2 \Delta\rho g}{3\eta\varphi[\phi(L')]} \tag{5}$$

where H is the height of the total oil + water mixture, L is the height of the resolved water (increasing with time), and $L' = L/H$. To model the time dependence of L, we need an expression for $\varphi[\phi(L')]$. This can be obtained using the Kozeny−Carman model as used in ref 17 which relates the hydrodynamic function φ to the drop volume fraction ϕ (for ϕ up to ≈ 0.75)

$$\varphi(\phi) = \frac{15\phi}{(1-\phi)^3} \tag{6}$$

In the region above the resolved water the drop volume fraction increases with time t due to the creaming. The oil volume remains constant but the emulsion-containing volume decreases. Hence we can write

$$\phi(L') = \frac{nV_\mathrm{d}}{V(L')} \tag{7}$$

where n and V_d are the drop number and volume, respectively. With $V(L')$ we denote the volume of the drop-containing space above the resolved water. Because L' increases, $V(L')$ decreases with time according to

$$V(L') = V_0(1 - L') \tag{8}$$

where V_o is the initial volume of the emulsion. Hence

$$\varphi[\phi(L')] = 15\left[\frac{\phi_0(1-L')^2}{(1-L'-\phi_0)^3}\right] \tag{9}$$

where ϕ_0 is the initial volume fraction (= 0.5). Introducing eq 9 into eq 5 and integrating, one obtains

$$15\phi_0\int_0^{L'}\frac{(1-L')^2}{(1-L'-\phi_0)^3}\,\mathrm{d}L' = \frac{a^2\Delta\rho g}{3\eta H}\int_0^t \mathrm{d}t \tag{10}$$

The initial condition accounts for the fact that no water is resolved at the moment $t = 0$. On integration we have

(15) Jansson, M.; Eriksson, L; Skagerlind, P. *Colloids Surf.* **1991**, *53*, 157.

(16) Happel, J.; Brenner, H. *Low Reynolds Number Hydrodynamics*; Prentice Hall: New Jersey, 1965.

(17) Petsev, D. N.; Starov, V. M.; Ivanov, I. B. *Colloids Surf.* **1993**, *81*, 65.

$$15\phi_0\left[\ln\left(\frac{1-\phi_0}{1-L'-\phi_0}\right)+\frac{4\phi_0(1-L'-\phi_0)+\phi_0^2}{2(1-L'-\phi_0)^2}-\frac{4\phi_0(1-\phi_0)+\phi_0^2}{2(1-\phi_0)^2}\right]=\frac{a^2\Delta\rho g}{3\eta H}t \quad (11)$$

Equation 11 relates the height of the resolved water L' with time t and has been used to model the water resolution at low electrolyte concentration. For our system, $\Delta\rho = 0.318$ g cm^{-3} and $\eta = 0.0089$ g s^{-1} cm^{-1} at 298 K. Fits of eq 11 to the creaming data for emulsions containing 0, 0.005, 0.01, and 0.015 M NaCl are shown in Figure 7 as lines. The experimental points are described very well using a time-independent drop radius a as a fitting parameter. The values of a determined by fitting (and given in the figure legend) are close to the average initial radii obtained from light diffraction measurements and change with salt concentration in the right direction. The fits to the data, however, may be fortuitous because non-hydrodynamic interactions, drop polydispersity, and the variation of radius with time are all neglected.

The curves in Figure 3 corresponding to higher electrolyte concentrations ($\geq$0.02 M) cannot be described by means of eq 11. They have a rather different shape indicating that the mechanism of creaming is not the same. For 0.02 M NaCl the creaming rate is much slower in the first 20 h compared with the curves at lower [NaCl]. After 20 h the creaming rate increases and becomes comparable. The situation is even more drastic at 0.025 M and above, where the creaming rate is practically zero until a certain time after which it increases, sometimes becoming greater than the low electrolyte cases. The induction time for creaming is maximum at 0.035 M NaCl. A possible reason for such behavior is that by increasing the salt concentration the electrostatic repulsion between the charged emulsion interfaces decreases and the drops start to attract each other. The attraction could lead to drop flocculation resulting in gel formation. The formation of a gel network is known to take place in emulsions even at much lower drop volume fractions, e.g., below 0.1.[18] In this case the viscous resistance upon buoyancy compression of the emulsion could be due mainly to energy dissipation within the thin liquid films formed between flocculated drops. Hence, it could be much greater than the resistance experienced by a single drop when moving upward even in the presence of other (nonflocculated) drops. This means that, during the induction time, slow rearrangements in the gel are probably taking place leading to more compact structures. After a certain time these structures become large enough to start moving rapidly upward, probably partially destroying the gel. A similar mechanism has been proposed by Manoj et al.[19] in explaining the delay period observed during the creaming of o/w emulsions stabilized by nonionic surfactant in the presence of a flocculant polymer. As soon as the drops flocculate the emulsion forms a space-filling structure which slowly rearranges until channels are formed that allow the flow of continuous phase to the base of the sample.

In addition to the effect of salt on the creaming described above, we seek to understand the reason for the change in the drop size with time seen in Figure 4. Because no free oil is resolved within the time scale of these experiments, we consider that the most likely mechanism for

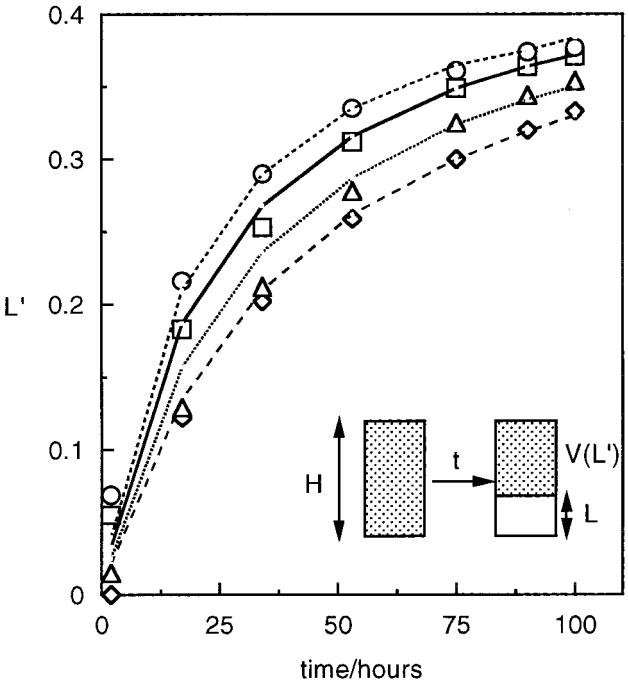

Figure 7. Resolution of water in terms of L' versus time for o/w emulsions at low salt concentration. The points are experimental and the lines are theoretical fits to eq 11 with a measured by light diffraction. The [NaCl]/M and fitted drop radii/μm, respectively, are 0, 4.4 (circles and small dashes); 0.005, 4.3 (squares and full line); 0.01, 3.7 (triangles and dotted line); and 0.015, 3.1 (diamonds and large dashes).

drop growth is Ostwald ripening and not coalescence. Ripening is the result of the solubility differences of the dispersed phase contained within drops of differing size. For o/w emulsions, the solubility within the continuous phase of oil in the form of spherical drops increases with decreasing size. As a consequence, oil contained within smaller drops tends to dissolve and diffuse through the aqueous phase recondensing onto larger drops. This results in an overall increase in the average size of the emulsion drops and an accompanying decrease in the interfacial area. The theory of the process was formulated by Lifshitz and Slezov[20] and independently by Wagner,[21] who derived the following equation for the rate of ripening, ω,

$$\omega = \frac{\mathrm{d}a_c^3}{\mathrm{d}t} = \frac{8c(\infty)\gamma V_m D}{9RT}f(\phi) \quad (12)$$

where a_c is the critical radius of a drop which at a given time is neither growing or dissolving, D is the diffusion coefficient of the dissolved species in the aqueous phase, V_m is the molar volume of the oil, $c(\infty)$ is the solubility of oil in an infinite sized drop, i.e., at a planar interface, and $f(\phi)$ is a correction coefficient taking into account the diffusional interaction of drops at finite values of ϕ (taken here equal to 2.8). The radius a_c may be reasonably approximated to the number average radius a_n of the drops. Experimental rates of Ostwald ripening, ω_e, can be obtained from the slopes of plots of the critical radius a_c cubed versus time if linear. In previous work concerned with ripening, a key question has been whether the solubility term $c(\infty)$ refers to the molecular solubility of oil or the enhanced solubility of oil contained within micelles, because micelles can potentially solubilize oil

(18) Bibette, J.; Mason, T. G.; Gang, H.; Weitz, D. A.; Poulin, P. *Langmuir* **1993**, *9*, 3352.
(19) Manoj, P.; Fillery-Travis, A. J.; Watson, A. D.; Hibberd, D. J.; Robins, M. M. *J. Colloid Interface Sci.* **1998**, *207*, 283.
(20) Lifshitz, I. M.; Slezov, V. V. *J. Phys. Chem. Solids* **1961**, *19*, 35.
(21) Wagner, C. Z. *Elecktrochem.* **1961**, *65*, 581.

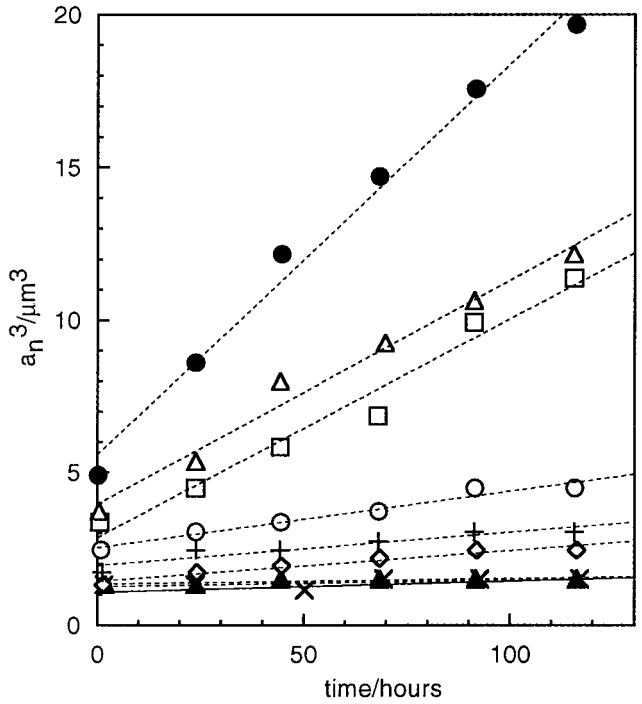

Figure 8. Cube of the number average radius versus time for o/w emulsions at low salt concentration. The [NaCl]/M are 0 (filled circles), 0.005 (open triangles), 0.01 (squares), 0.015 (open circles), 0.02 (crosses, +), 0.025 (diamonds), 0.03 (crosses, x), and 0.035 (filled triangles).

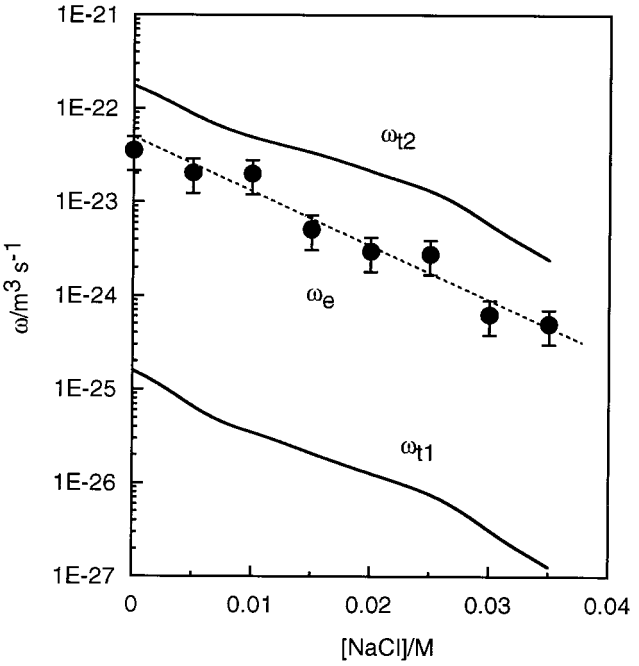

Figure 9. Experimental Ostwald ripening rates, ω_e, as a function of salt concentration for heptane-in-water emulsions stabilized by AOT. Theoretical rates calculated using eq 12 refer to the molecular solubility of heptane (ω_{t1}) or the micellar solubility (ω_{t2}).

from emulsion drops and act as carriers. Kabalnov and others[22−24] report that ω_e is virtually independent of the micelle concentration for alkane-in-water emulsions stabilized by sodium dodecyl sulfate (SDS), with ω_e agreeing reasonably well with the theoretical value ω_{t1} if the molecular solubility of the oil in water is used in eq 12. It is argued that due to electrostatic repulsion, SDS micelles cannot absorb oil directly from emulsion drops. In contrast, ω_e increases with micelle concentration for decane-in-water emulsions of a nonionic surfactant ($C_{12}E_6$) capable of substantial solubilization of oil.[25]

Figure 8 shows plots of a_n^3 with time for heptane-in-water emulsions stabilized by AOT at low salt concentrations. The plots are fairly linear as predicted by eq 12. As seen in Figure 9, ω_e decreases by nearly 2 orders of magnitude upon increasing the salt concentration and by 0.03 M NaCl ripening is virtually absent, due mainly to the drastic lowering of the interfacial tension γ. If aqueous micelles act as carriers for oil between emulsion drops, values of ω_{t2} have been obtained as follows. Although the initial concentration of AOT in water is 40 mM, we estimate from the emulsion drop sizes that approximately 5 mM is required to cover the interfaces around drops leaving 35 mM surfactant capable of forming micelles in the continuous phase. Such micelles solubilize heptane to an extent denoted by R_0 = [heptane]/[AOT] which increases markedly with salt concentration.[26] The values of $c(\infty)$ required originate from a knowledge of the R_o value and the molar volume of heptane. The drop size dependence of the diffusion coefficient of heptane D in micellar form has also been taken into account (Table 1). The correspondence between values for ω_e and ω_{t2} to within a factor of 6 implies that micelles act as carriers of oil in this system if no energy barrier exists for this process. By contrast, values of ω_{t1} are around 2 orders of magnitude lower than ω_e values.

Table 1. Parameters Required To Determine Theoretical and Experimental Ostwald Ripening Rates, and Zeta Potentials, as a Function of Salt Concentration for Heptane-in-Water Emulsions Stabilized by AOT at 25 °C

[NaCl] (M)	R_0[a]	$10^3\gamma$ (N m^{-1})	$10^{10}D$[b] (m^2 s^{-1})	$10^3c(\infty)$[c] (m^3 m^{-3})	$-\zeta$ (mV)
0	0.8	2.50	11.6	4.10	99
0.005	1.2	1.05	9.15	6.15	105
0.01	1.5	0.55	7.91	7.69	101
0.015	2.4	0.33	5.62	12.30	83
0.02	2.9	0.20	4.84	14.90	81
0.025	3.4	0.12	4.26	17.40	79
0.03	5	0.05	3.06	25.60	74
0.035	7.8	0.02	2.06	40.00	77

[a] R_0 = [heptane]/[AOT] in micelles, taken from ref 26. [b] Calculated from the Stokes−Einstein equation taking into account the increasing micelle size with [NaCl]. [c] Total solubility of heptane in water, calculated from the R_0 value and the molar volume V_m (= 1.47×10^{-4} m^3 mol^{-1}).

To confirm that Ostwald ripening occurs in these emulsions, we investigated the effect of adding a small quantity (1 vol % in heptane) of a longer chain alkane in the oil phase in order to arrest the process completely. The argument follows from the work of Higuchi and Misra,[27] who showed that if one of the components of a two-component miscible dispersed phase is less soluble in the continuous phase than the other component, small amounts of such a substance may stop the ripening. This is because the mass transfer of the more soluble component from small to large drops changes their composition. It results in an increased concentration of the less soluble

(22) Kabalnov, A. S. *Langmuir* **1994**, *10*, 680.
(23) Taylor, P. *Colloids Surf. A* **1995**, *99*, 175.
(24) Soma, J.; Papadopoulos, K. D. *J. Colloid Interface Sci.* **1996**, *181*, 225.
(25) Binks, B. P.; Clint, J. H.; Fletcher, P. D. I.; Rippon, S.; Lubetkin, S. D.; Mulqueen, P. J. *Langmuir* **1999**, *15*, 4495.
(26) Fletcher, P. D. I. *J. Chem. Soc., Faraday Trans. 1* **1987**, *83*, 1493.
(27) Higuchi, W. I.; Misra, J. *J. Pharm. Sci.* **1962**, *51*, 459.

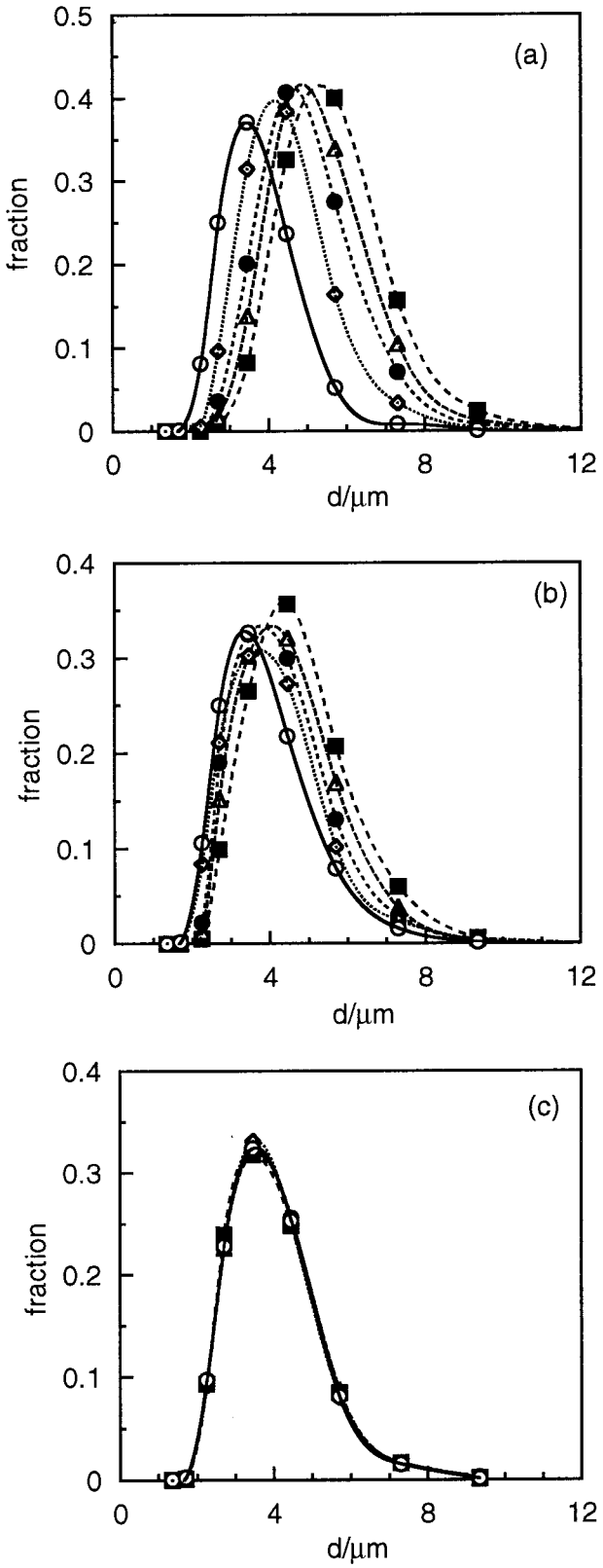

Figure 10. Changes in the number average drop diameter distributions with time for various o/w emulsions without added salt. Emulsion ages/h are 0.2 (open circles), 24 (diamonds), 45 (filled circles), 68 (triangles), and 92 (squares). (a) Heptane; (b) heptane + 1 vol % undecane; (c) heptane + 1 vol % tetradecane.

component in the small drops and a decreased concentration in the larger ones. This leads to a compensation of the difference in chemical potential of the more soluble component caused by the difference in capillary pressures.

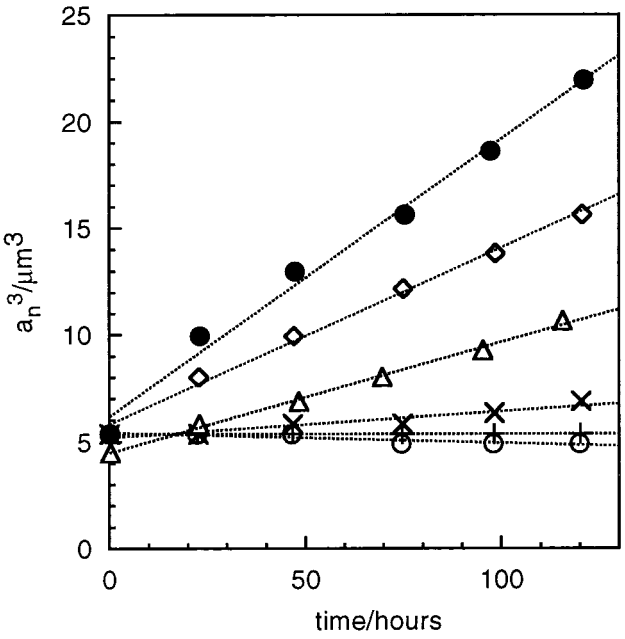

Figure 11. Cube of the number average radius versus time for o/w emulsions with no added salt containing heptane + 1 vol % of higher alkanes. The points are C_7 (filled circles), + C_{10} (diamonds), + C_{11} (triangles), + C_{12} (crosses, x), + C_{14} (crosses, +), + C_{16} (open circles).

When the capillary and concentration effects completely compensate, the mass transfer terminates and the drops come to "equilibrium". The profound effect of adding a longer alkane to heptane-in-water emulsions is seen from the time-dependent drop size distributions in Figure 10 for the case of no added salt, i.e., where ripening is relatively rapid for pure heptane. The extent of ripening is reduced on addition of undecane and is more or less zero in the presence of tetradecane, whose solubility in pure water or aqueous AOT solutions is much lower than that of heptane. In Figure 11 we show the linear plots of a_n^3 against time for the admixtures with several alkanes from decane to hexadecane. The rates of ripening ω_e fall to very low values once the chain length of the minor component reaches 12, supporting our idea that Ostwald ripening is the cause of the coarsening in drop size in pure heptane emulsions.

(c) Stability at High [NaCl], ≥ 0.035 M. To understand why significant coalescence occurs at higher salt concentrations, we analyze the energy of interdrop interaction as a function of salt concentration. Drop deformability, due to attractive interactions and increased by a low interfacial tension, is taken into account using the theory developed by Danov et al.[10,11] We calculate the interaction energy between two deformed oil drops of initial radius a separated by a plane parallel water film of thickness h. As a reference, a system of two nondeformed spherical drops at infinite separation is used. The deformation is assumed to occur at constant volume of the drops. The total interaction energy $W(h,r)$ between two deformed drops can be presented as a sum of different contributions

$$W(h,r) = W_e(h,r) + W_{vdW}(h,r) + W_s(r) \qquad (13)$$

with

$$W_e(h,r) = \frac{64\pi c_{el} kT}{\kappa} \tanh^2\left(\frac{e\psi_0}{4kT}\right) \exp(-\kappa h)\left(r^2 + \frac{a}{\kappa}\right) \qquad (14)$$

being the electrostatic repulsion term for weakly overlap-

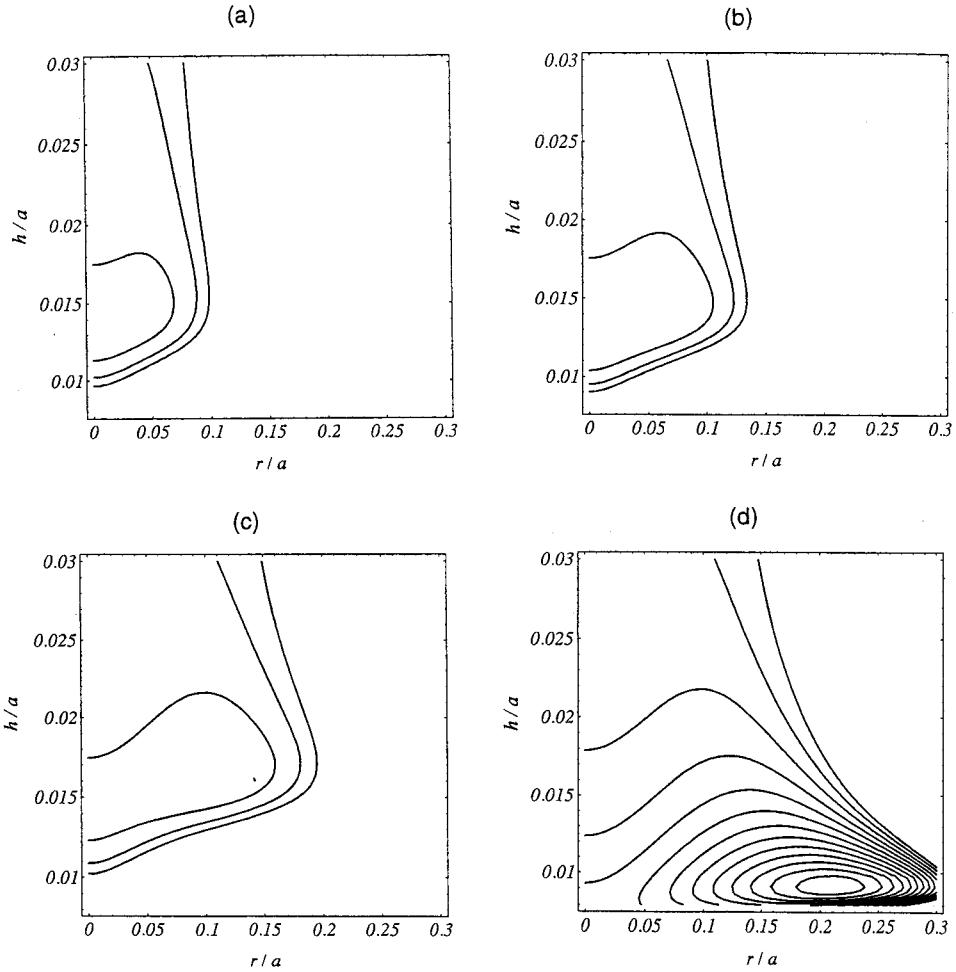

Figure 12. Contour diagrams of the interdrop interaction energy $W(r,h)/kT$ as a function of the film radius (r) and film thickness (h) relative to the drop radius (a) for different salt concentrations. Only the negative energy values are plotted and the outermost corresponds to zero energy. The distance between two adjacent contours is 2 kT. (a) [NaCl] = 0.025 M, a = 1.30 μm, γ = 0.11 mN m^{-1}, ψ_o = −77.5 mV.(b) [NaCl] = 0.03 M, a = 1.25 μm, γ = 0.05 mN m^{-1}, ψ_o = −71.6 mV.(c) [NaCl] = 0.035 M, a = 1.02 μm, γ = 0.021 mN m^{-1}, ψ_o = −75.2 mV.(d) [NaCl] = 0.04 M, a = 1.80 μm, γ = 0.007 mN m^{-1}, ψ_o = −78.4 mV.

ping double layers ($\kappa a \gg 1$, $\kappa h \gg 1$, but $h/a \ll 1$) in which ψ_0 is the surface potential of the drops. The van der Waals attractive energy is given by

$$W_{vdW}(h,r) = -\frac{A}{12}\left\{\frac{4a^2}{(2a+h)^2} + \frac{4a^2}{h(4a+h)} + 2\ln\left[\frac{h(4a+h)}{(2a+h)^2}\right] + \frac{128a^5r^2}{h^2(2a+h)^3(4a+h)^2}\right\} \quad (15)$$

where A is the Hamaker constant for the interaction of dispersed oil across an aqueous film. Equation 15 contains contributions from the energy of the spherical parts of the drops and the energy of the flat film between them. The surface deformation energy, $W_s(r)$, accounts for the increase in interfacial area due to the deformation. Assuming that the adsorption of surfactant is fast enough, the interfacial tension γ remains constant during deformation. In other words the Gibbs elasticity is zero and

$$W_s(r) = \frac{\pi\gamma r^4}{2a^2} \quad (16)$$

i.e., it acts like a soft repulsion. Equations 14−16 hold for moderately deformed drops, i.e., $(r/a)^2 < 0.1$.

Using the approach outlined briefly above, we can calculate the energy of interdrop interaction accounting for the specific features distinguishing emulsion drops (especially with low interfacial tension) from solid particles. All of the parameters needed for the calculations are taken from the literature or from experiments described earlier. They include the drop radius a, the surface potential ψ_0 (assumed to be equal to the ζ potential), the interfacial tension γ, and $A = 4 \times 10^{-21}$ J from ref 28. Introducing these parameters into eqs 13−16 enables the contour diagrams of the interaction energy as a function of film thickness h and film radius r to be obtained. These are presented in Figure 12 for four electrolyte concentrations. Starting from the lowest concentration, one sees that there is almost no deformation or film formation, but with increasing concentration the deformation and the interdrop attraction increase. Thus, for 0.025 M (a) the drops interact as non-deformable spheres, the film radius is practically zero, and the attractive well has a depth of −4.84 kT. At 0.03 M (b) we can begin to distinguish the cases where the deformation is taken into account or neglected. In the former the attractive energy is −5.38 kT which corresponds to a film radius r/a = 0.063, while the reference hard sphere interaction (which is along the ordinate axis at r = 0) gives −5.14 kT. However, the difference between the energies is not large and the film radius is small. For a

(28) Israelachvili, J. N. *Intermolecular and Surface Forces*, 2nd ed.; Academic Press: London, 1991.

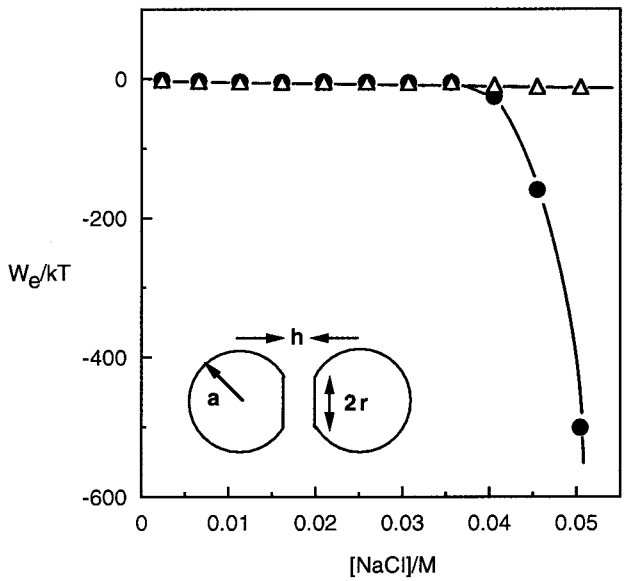

Figure 13. Depth of the attractive energy secondary minimum W_e (r_e, h_e)/kT versus electrolyte concentration. Open triangles are for $r = 0$ (no deformation), filled circles are for $r = f$(NaCl), i.e., with deformation. Each point is calculated with experimentally determined parameters.

salt concentration equal to 0.035 M (c) the film radius increases to $r/a = 0.111$ and the difference in the attractive energy between deformed and non-deformed drops becomes almost 1 kT (−5.42 and −4.51 kT respectively). Hence, up to these salt concentrations, the attraction is sufficient to allow drop flocculation and eventually gel formation although film formation is not particularly favored. Changing the salt concentration to 0.04 M, however, has an extreme impact on the emulsion stability. Experimentally it is seen that the induction time for creaming starts to decrease and oil resolution resulting from coalescence occurs. This may be viewed as coalescence occurring in the creamed emulsion leading to the appearance of free oil above it and water beneath it. The calculations in (d) are in qualitative agreement with such a notion. The energy minimum for the interaction between two deformed drops is $W_e(h_e, r_e)/kT = -25.32$ and the relative deformation $r/a = 0.211$. The deformed configuration at this condition is much more favorable than if no deformation was present. In the latter case $W_e(h_e, r_e)/kT = -9.03$, which is about 2.5 times less. It is not surprising that such strong attraction may facilitate coalescence.

A more detailed illustration of the interaction energy minimum dependence on electrolyte concentration is shown in Figure 13. Each point is calculated using parameters measured at the respective electrolyte concentration. The attractive well is the same for deformable and nondeformable drops up to [NaCl] = 0.025 M, starting from $W_e(h_e, r_e)/kT = -1.68$ at 0 M and reaching −4.84 at 0.025 M. The difference is still not very great at the critical value of 0.035 M, but beyond this point the drops become much more attractive and deformable. At 0.045 M, $W_e(h_e, r_e)/kT = -159.0$ and $r/a = 0.524$ for the deformable case, compared with −11.5 for the attractive well when no deformation takes place. These differences increase sharply with the electrolyte concentration. One reason for such a trend with salt concentration is certainly the charge screening which enhances the attraction between drops. More important, however, is the decrease in the interfacial tension (appearing in eq 16) which changes from 0.12 mN m^{-1} for 0.025 M NaCl to 0.007 mN m^{-1} for 0.04 M. It appears that up to 0.035 M NaCl, attraction is present and can lead to gelation of the emulsion although the deformation is not substantial. At 0.035 M and above, the film formation and interdrop attraction increase strongly and may lead to coalescence.

Conclusions

We studied in detail the effect of electrolyte concentration on the stability of o/w emulsions of AOT prepared from equilibrium o/w microemulsions and their excess oil phases. The stability to creaming passes though a maximum around 0.035 M NaCl, well before the salt concentration required for three-phase formation (0.055 M). Below 0.035 M, the emulsions are stable to coalescence but coalescence becomes more extensive above this concentration leading to very unstable emulsions near the Winsor I/III boundary. We account for the behavior at low salt concentrations in terms of creaming enhanced by Ostwald ripening. Experimental ripening rates indicate that heptane is transported via o/w microemulsion drops present in the aqueous continuous phase. The behavior at higher salt concentrations is described in terms of creaming enhanced by coalescence. Calculations of the attractive pair interaction energy between two drops are consistent with these observations and show that, because of a significant lowering of interfacial tension in this system with salt concentration, the deformation of drops can occur resulting in attraction and instability.

Acknowledgment. We thank LG Chemicals Ltd. (South Korea) for the award of a studentship to W-G.C.

LA990952M